

Effect of Cu on Optical Properties of TiO₂ Nanoparticles

Realpe Jiménez Álvaro, Núñez D. Diana and Acevedo Morantes María

Department of Chemical Engineering, Research Group of Modeling of Particles
and Processes, University of Cartagena, Av. Consulado No. 48 – 152
Cartagena, Colombia

Copyright © 2017 Realpe Jiménez Álvaro, Núñez D. Diana and Acevedo Morantes María. This article is distributed under the Creative Commons Attribution License, which permits unrestricted use, distribution, and reproduction in any medium, provided the original work is properly cited.

Abstract

Cu-doped TiO₂ nanoparticles were prepared; the effect of Cu on optical properties of TiO₂ nanoparticles to shift its absorption edge toward visible light region was studied. By using a green synthesis mechanism were obtained TiO₂ nanoparticles, and through wet - impregnation method using copper sulfate as precursor were obtained Cu-TiO₂ nanoparticles. The synthesized material was characterized by Fourier transform infrared spectroscopy (FT-IR), Scanning electron microscopy (SEM), Energy Dispersive Spectroscopy (EDS), UV-VIS diffuse reflectance spectroscopy (UV-Vis/RDS). FTIR characterization have been made to confirm the formation of TiO₂. Through EDS analysis was determined the ion dopant percent in each sample. Morphological properties and particle size were identified by SEM micrographs, which disclose a spherical shape with an average size between 70 and 27.3 nm. UV-VIS/RDS spectrum showed that the band gap energy decreases with the increase of Cu concentration in TiO₂, for that reason, doped nanoparticles had activity under visible light irradiation.

Keywords: Titanium dioxide, doping, band gap, UV- light, visible light

1 Introduction

Titanium dioxide is a photosensitive semiconductor, it can be excited to produce electron-hole pair under ultraviolet light irradiation, through photoinduced processes that take place in TiO₂ [1]. Due to its chemical stability, non-toxicity, high photochemical resistance and abundance, has attracted a lot of interest in the scientific community [2]. It has been widely researched and numerous applications

have been developed in different areas, including photocatalysis, photovoltaic and photoelectrochemical devices and painting industry [3-5]. Photoinduced processes on TiO₂ are originated from its band gap (E_g), when photons emitted by a light source have a higher energy than band gap energy of TiO₂, they are absorbed and an electron (e⁻) is promoted from the valence band to the conduction band, leaving a hole (h⁺) in the valence band [6]. The photoexcited electron can be used directly to produce electricity in photovoltaic solar cells or to drive chemical reactions.

TiO₂ is a semiconductor with a large band gap, E_g = 3.2 eV and 3.0 eV for more common polymorphs of TiO₂ rutile and anatase, respectively [6-7], due to this, photoinduced reactions in TiO₂ take place under ultraviolet irradiation at 387 nm [8], which comprises around 3-5 % of solar light energy. To overcome this limitation, different ways have been investigated to extend its activity to visible region, making a better use of solar resource. Modification of electronic structure (doped) through insertion of non-metal ions, transition metal ions or rare earth elements has been an important alternative [6-9]. Metal transition doped has demonstrated to be an effective alternative to reduce the band gap of TiO₂ because it creates impurity levels that allow the electronic transitions within the conduction band and valence band, and simultaneously reduces the recombination rate of photogenerated charges [10]. In water photoelectrolysis, extending the TiO₂ photoresponse from the ultraviolet to the visible light region using Fe, Co, Mn, and Cu has been reported [11-13], leading also the increase of photocurrent density and the incident photon to current efficiency (IPCE) in relation to non-doped material [12].

This work aims to reduce the band gap energy of TiO₂ nanoparticles obtained from a green synthesis mechanism based on the Lemon Grass extract, in which organic solvents are replaced and natural extracts are used as reducing agent of the precursor alcoxide. Through impregnation wet were doped TiO₂ nanoparticles with copper sulfate as an ion precursor and their potential use under visible light irradiation was investigated.

2 Materials and Methods

2.1 Materials

Pure TiO₂ nanoparticles obtained from a green synthesis mechanism based on the Lemon Grass extract. Titanium isopropoxide IV (C₁₂H₂₈O₄Ti) – 95%, manufactured by AlfaAesar was used as a TiO₂ precursor, ethanol (CH₃CH₂OH) manufactured by Panreac was used for washing nanoparticles. Copper sulfate pentahydrate (CuSO₄ · 5H₂O) was used as a source of Cu for doping.

2.2 Synthesis of Titanium Dioxide Nanoparticles

Fresh leaves of Lemon Grass (*Cymbopogon Cytratus*) were washed with distilled water to remove the dust or any other dirt of the environment and dried at 40°C in a furnace, after that the leaves were cut into fine pieces and grinded. Aqueous extract was prepared by immersion of 100 g of lemon grass in 500 ml of distilled water at 90°C. This extract was filtered several times and concentrated by

evaporation heating it at 60°C. For synthesis of pure TiO₂ nanoparticles, an aqueous solution of 5mM of titanium isopropoxide was stirred by ultrasound during 30 min, 15 ml of the aqueous extract of lemon grass was added in 85 ml of isopropoxide solution with continuous stirring at 175 rpm and room temperature for 24 h [14]. After the reduction reaction, nanoparticles synthesized were removed by centrifugation and dispersed in ethanol and then in distilled water to wash out impurities. Finally, TiO₂ nanoparticles were dried in an oven at 100°C and then they were calcined in a muffle furnace for 3 h, starting at 300°C until 550°C, this heat treatment also allows the removal of organic matter without reacting [15].

2.3 Preparation of Fe doped TiO₂ Nanoparticles

TiO₂ nanoparticles were doped by using wet impregnation method [10]. Wet impregnation is a used technique where the precursor material is dissolved in a solvent and mixed with the support, and then the solvent is removed by evaporation when the precursor gets deposited on the bas material. An amount of TiO₂ was added in distilled water, the TiO₂ slurry was stirred (by ultrasound) for 30 min (to break up the loosely attached aggregates). After, an aqueous solution of Copper sulfate pentahydrate (precursor of Cu) with the required amount of precursor for doping was added to TiO₂ suspension (1, 3, and 5 wt % of copper was introduced as the dopant). It was subject of stirring by ultrasound at room ambient during 1 h, and subsequently stirring with heating at 60°C to evaporate the solvent, dried at 120°C and finally doped nanoparticles were calcined in a muffle furnace at 400°C for 1 h.

2.4 Characterization methods

The FTIR spectra of the samples, in the range of 400 to 4000 cm⁻¹, were recorded as the percentage of transmittance (%T) versus wavenumber. This analytic method is useful for the determination of the functional groups present in the nanoparticles synthesized identified by its characteristic peaks in the spectrum. The morphology, dimension and surface characteristics of the TiO₂ nanoparticles synthesized were determined with a scanning electron microscopy, Tescan model Vega 3, the sample was analyzed at 18°C. Determination of Cu presence and the chemical composition in TiO₂ samples were determined by using Energy Dispersive X-ray Spectroscopy, the amount of Cu introduced into the structures as a percentage of mass of Cu in relation to the mass of TiO₂ may be obtained with this. This analysis was carried out using a scanning electron microscope with a probe EDX Bruker Nano GmbH Berlin. The optical measurements were carried out to determine the band gap of pure TiO₂ and Cu doped TiO₂ to recognize the relative position of the absorption edge as an important indication whether the absorption edge has been shifted toward visible region, to find a relationship between the band gap energy and the amount of Cu used for doping the semiconductor.

UV-Vis spectroscopy in mode diffuse reflectance spectra were recorded on a spectrophotometer UV/VIS Evolution 600 Thermo Scientific in the wavelength range of 200 to 800 nm.

3 Results and Discussions

3.1 Fourier Transform Infrared – FTIR

FTIR analysis was performed to identify the role of the lemon grass leaf extract in the reduction reaction to produce titanium dioxide nanoparticles. Figure 1 shows the infrared spectra of green synthesized TiO₂. In Figure 1.a, a broad band located at 3278.98 cm⁻¹ is observed, which is assigned to the stretching vibration of the hydroxyl bond (-OH) and the band around 1630 cm⁻¹ is attributed to the bending mode of hydroxyl vibrations (-OH), this vibration band is related to protons of the physisorbed water into the synthesized material [16]. According to [17] titanium oxide retains adsorbed undissociated water due to the strong Lewis acidity of the co-ordinatively unsaturated Ti⁴⁺ surface sites. The descent band absorption at 1000 - 400 cm⁻¹ is due to vibration modes of Ti-O, which indicates the formation of TiO₂ [16-17]. The chemical bonding of the Cu doped TiO₂ nanoparticles were also scrutinized. Figure 1.b, shows the IR spectra of the Cu/TiO₂ nanoparticles, all the doped samples show similar spectra to pure TiO₂, the intensities of these signals decrease according to undoped TiO₂, indicating water desorbed [18]. It is not detected bands in the low frequency regions that can be attributed to Cu-O vibration bond [19]. The absence of evidence of oxides generated from the dopant implies that the ions were incorporated within the TiO₂ lattice.

3.2 Scanning Electron Microscopy – SEM

The size and morphology of the nanoparticles with different contents of Cu-TiO₂ were determined by a scanning electron spectroscopy (SEM). The SEM image of pure and doped TiO₂ are presented in Figure 2a-d. The morphology is not uniform in these samples but prevails spherical shape in the nanoparticles. The particle size is not uniform for pure and doped TiO₂ nanoparticles, and there is a propensity to form aggregates, especially in Cu doped TiO₂, according to [20], the temperature of calcination affects the size and agglomeration of crystalline particles. The particle size was measured by using ImageJ software, for pure TiO₂ 70 nm was determined, conversely, Cu doping produced a decreased in the particle size around 27.3 nm – 28.5 nm. These results are in agreement with the results obtained by [21], in this investigation the decrease in the particles size of commercial Degussa P-25 TiO₂ is attributed to the suppression of particle growth by the introduction of Cu atoms into the TiO₂ crystal structure.

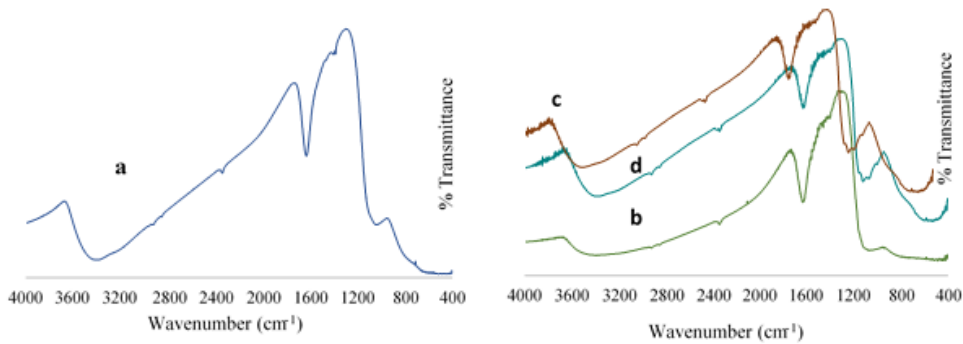


Figure 1. FTIR spectrum of pure TiO₂ nanoparticles synthesized, (a) pure TiO₂, (b) 1% wt Cu doped TiO₂, (c) 3% wt Cu doped TiO₂, (d) 5% wt Cu doped TiO₂

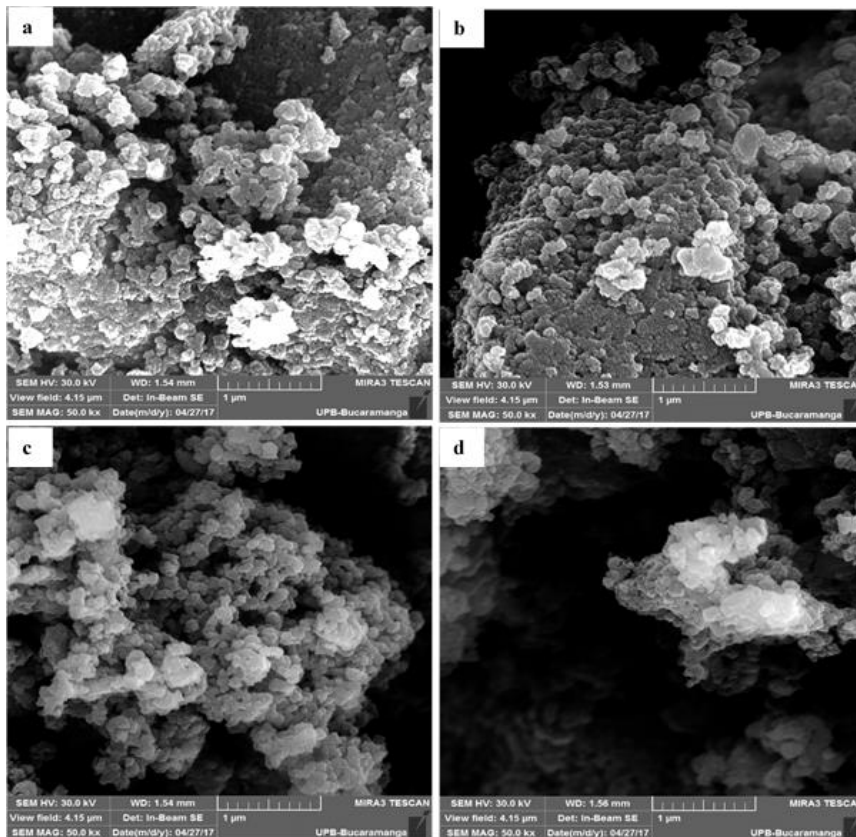


Figure 2. SEM micrographs of TiO₂ synthesized, a. Pure TiO₂, b. 1% wt Cu doped TiO₂, c. 3% wt Cu doped TiO₂, d. 5% wt Cu doped TiO₂

3.3 Dispersive X-ray Spectroscopy – EDS

Figure 3 shows the elemental composition of each sample evaluated through energy dispersive X-ray spectroscopy. In these spectrum, the characteristic X ray energy emitted from Ti are observed on 4.508 (K α) and 0.452 (L α) keV, and O are on 0.525 (K α) keV, in doped samples the characteristic signals of Cu are observed

on 8.040 ($K\alpha$) and 0.930 ($L\alpha$) keV [22]. In doped samples, the presence of S is identified on 2.307($K\alpha$) keV, which is due to the CuSO_4 used by the Cu precursor [23]. There are peaks associated with K ($K\alpha$), Ca ($K\alpha$), Mg ($K\alpha$), Si ($K\alpha$) and P ($K\alpha$); these lines are attributed to the equipment used for the analysis or impurities (Varma et al, 2014). The percentage real of Cu incorporated into the TiO_2 structure was 0.78, 2.98 and 4.59% wt., with respect to the initial amount of Cu added during the doping process 1, 3 and 5% wt., so the amount of impregnated material was similar as was taken for impregnation.

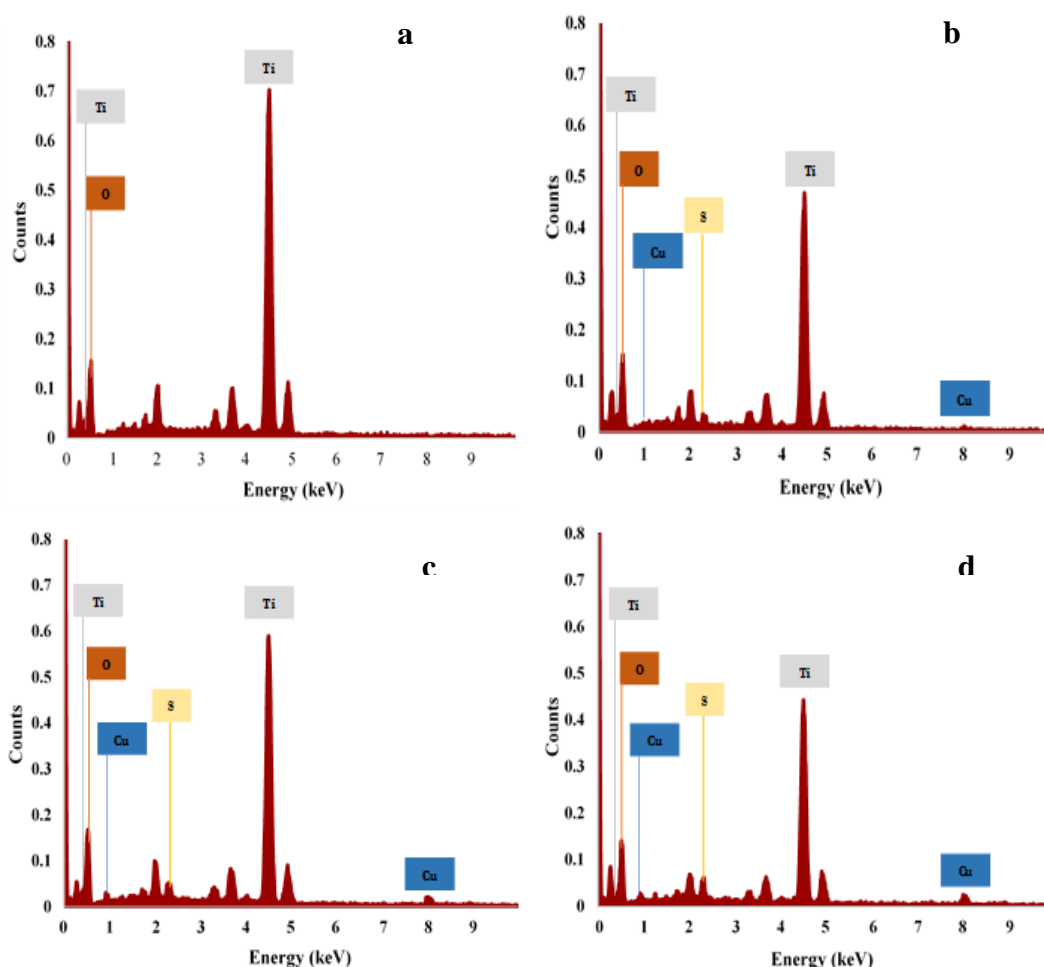


Figure 3. Energy Dispersive X-ray Spectroscopy spectrum, a. Pure TiO_2 , b. 1% wt Cu doped TiO_2 , c. 3% wt Cu doped TiO_2 , d. 5% wt Cu doped TiO_2

3.4 UV-VIS Diffuse Reflectance Spectroscopy – UV-VIS/DRS

The UV-VIS/RDS spectra of pure and doped TiO_2 are depicted in Figure 4. The optical electronic excitation from valence band to conduction band is generally showed through an increase in the absorbance band in a specific wavelength in a UV-VIS spectrum [24]. All samples in this figure have a sharp absorption band in the region comprised by wavelength less than 400 nm, which may be attributed to

the band structure of original TiO₂. However in doped samples is observed the increase of the absorbance in wavelengths higher than 400 nm, therefore, the valence band in doped samples can be excited with photons of lower energy than pure TiO₂. Figure 4 reveals that incorporation of copper ions leads to shift of optical response toward visible region of the spectra, in the same way, increasing the amount of dopant, increases the intensity of those absorbance peaks in the visible region. Based on the spectrum in figure 4, the optical energy band gap of pure TiO₂ and Cu doped TiO₂ was determined by using the Tauc plot relation. Starting with the equation $\alpha h\nu = B(h\nu - E_g)^n$, where α is the absorption coefficient, which is proportional to the absorbance, h is the Planck's constant (J.s), ν is the light frequency (s⁻¹), B is the absorption constant, E_g the band gap energy and n is a constant related to the electronic interband transition. $n = 2$ for an indirect allowed transition (plotted as $(\alpha h\nu)^{1/2}$ versus E), $n = 3$ for an indirect forbidden transition (plotted as $(\alpha h\nu)^{1/3}$ versus E), $n = 1/2$ for a direct allowed transition (plotted as $(\alpha h\nu)^2$ versus E), $n = 3/2$ for a direct forbidden transition (plotted as $(\alpha h\nu)^{2/3}$ versus E) [24]. Plotting $(\alpha h\nu)^{1/n}$ as a function of E (photon energy), the band gap energy value is obtained by extrapolating until $(\alpha h\nu)^{1/n} = 0$ the linear section of this spectra. Considering in TiO₂ an indirect allowed transition, the band gap energy obtained for pure TiO₂ and doped TiO₂ samples are plotted on Figure 5.

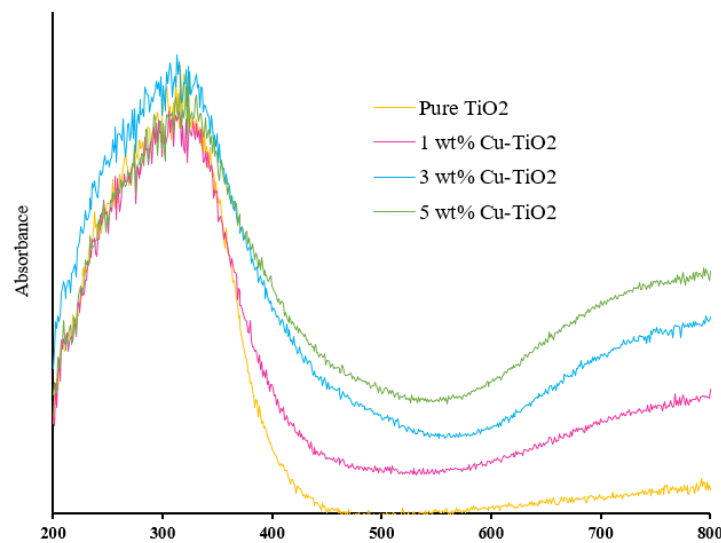


Figure 4. UV-VIS/RDS spectrum of TiO₂ samples

Figure 5 illustrates the estimation of band gap energy for all samples by extrapolation the straight line to the E (eV) axis. The band gap energy (E_g) obtained for TiO₂ nanoparticles synthesized by green synthesis method is 2.98 eV, the calculated E_g values for Cu doped TiO₂ with 1%, 3%, and 5% are 2.6 eV, 2.23 eV and 1.99 eV, respectively. Figure 5 shows that the band gap energy decreases with Cu doping and with the increasing of the Cu concentration, furthermore, these results suggest that Cu doping certainly causing absorbance of visible light by TiO₂.

The band gap energy values obtained in this investigation are similar to those reported by [25], in which have reported a reduction in band gap of TiO_2 from 3 eV for pure samples to 1.6 eV for 7.5 % Cu doped TiO_2 by using a different doping mechanism. Doping with transition metals can extend the absorption edge of TiO_2 to visible light due to its electronic characteristics, through inserting new electronic states into the original band gap, which is why electrons can be excited from the defect state to the TiO_2 conduction band by photons less energy [26]. According to the work developed by Guo and Du [27], Cu doping can induce some doping states near the top of valance band, and thus enhance the visible absorption in the range of 400–1000 nm by Cu 3d–Ti 3d optical transition.

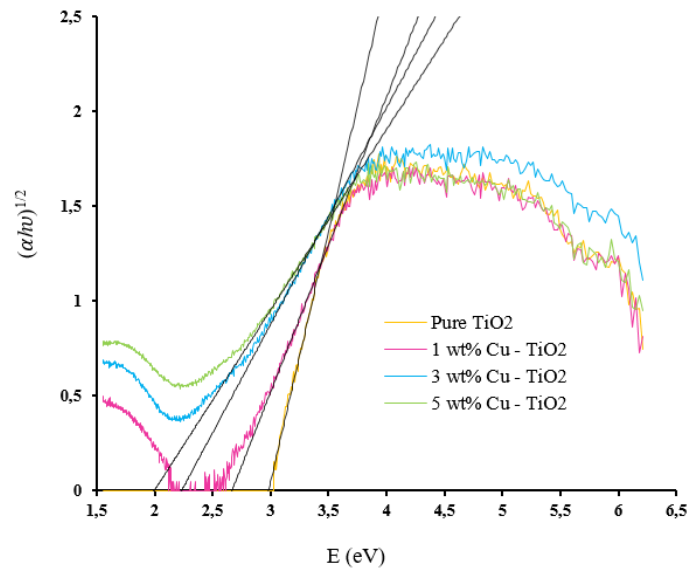


Figure 5. Tauc plot of pure TiO_2 and doped TiO_2

4 Conclusions

Titanium dioxide and Cu doped TiO_2 particles have been synthesized, the biosynthesis mechanism led to obtain particles with nanometric size. The size decreased in Cu doped TiO_2 nanoparticles. The metal doping in titanium dioxide has been carried out by wet impregnation process, Cu doped TiO_2 showed a reduction in the band gap from 2.98 eV to 1.99 eV, shifting the absorption edge of TiO_2 toward a region of lower energy, which improve the photoactive process in the material.

Acknowledgements. Authors of this paper would like to express their gratitude to University of Cartagena for providing the recourses and the space to perform this project through the resolution No. 031-2017.

References

- [1] L. Bedikyan, S. Zakhariyev, M. Zakhariyeva, Titanium dioxide thin films: preparation and optical properties, *J. Chem. Technol. Metal.*, **48** (2013), no. 6, 555–558.
- [2] T.E. Agustina, R. Komala, M. Faizal, Application of TiO₂ nano particles photocatalyst to degrade synthetic dye wastewater under solar irradiation, *Contemporary Engineering Sciences*, **8** (2015), no. 34, 1625-1636.
<https://doi.org/10.12988/ces.2015.511305>
- [3] A. Realpe, D. Núñez, I. Carbal, M. Acevedo, G. De Ávila, Preparation and Characterization of Titanium Dioxide Photoelectrodes for Generation of Hydrogen by Photoelectrochemical Water Splitting, *International Journal of Engineering and Technology*, **7** (2015), no. 2, 753-759.
- [4] X. Chen, S.S. Mao, Titanium dioxide nanomaterials: Synthesis, properties, modifications and applications, *Chem Rev.*, **107** (2007), no. 7, 2891–959.
<https://doi.org/10.1021/cr0500535>
- [5] Á. Realpe, D. Núñez, M. Acevedo, Effect of pH on Photovoltage Behavior of TiO₂ Photoanodes, *International Journal of Engineering and Technology*, **9** (2017), no. 1, 175-178. <https://doi.org/10.21817/ijet/2017/v9i1/170901419>
- [6] D.M. Tobaldi, Š.A. Sever, R.C. Pullar, M.P. Seabra, J.A. Labrincha, Titanium dioxide modified with transition metals and rare earth elements: Phase composition, optical properties, and photocatalytic activity, *Ceramics International*, **39** (2013), no. 3, 2619–2629.
<https://doi.org/10.1016/j.ceramint.2012.09.027>
- [7] Z. Shi, X. Wen, Z. Guan, D. Cao, W. Luo, Z. Zou, Recent progress in photoelectrochemical water splitting for solar hydrogen production, *Annals Physics*, **358** (2015), 236–247. <https://doi.org/10.1016/j.aop.2015.04.005>
- [8] R. Hussin, K.L. Choy, X. Hou, Deposited TiO₂ thin films by atomic layer deposition (ALD) for optical properties, *ARPJ Journal of Engineering and Applied Sciences*, **11** (2016), no. 12, 7529-7533.
- [9] M. Kralova, P. Dzik, M. Vesely, J. Cihlar, Preparation and characterization of doped titanium dioxide printed layers, *Catal. Today*, **230** (2014), 188–196.
<https://doi.org/10.1016/j.cattod.2013.09.018>
- [10] L.S. Yoong, F.K. Chong, B.K. Dutta, Development of copper-doped TiO₂ photocatalyst for hydrogen production under visible light, *Energy*, **34** (2009), no. 10, 1652–1661. <https://doi.org/10.1016/j.energy.2009.07.024>

- [11] Á. Realpe, D. Núñez, I. Carbal, M. Acevedo, Sensitization of TiO₂ Photoelectrodes Using Copper Phthalocyanine for Hydrogen Production, *International Journal of Engineering and Technology*, **7** (2015), no. 4, 1189-1193.
- [12] C. Wang, Z. Chen, H. Jin, C. Cao, J. Li, Z. Mi, Enhancing visible-light photoelectrochemical water splitting through transition-metal doped TiO₂ nanorod arrays, *J. Mater. Chem. A*, **2** (2014), no. 42, 17820-17827. <https://doi.org/10.1039/c4ta04254a>
- [13] Á. Realpe, D. Núñez, A. Herrera, Synthesis of Fe-TiO₂ Nanoparticles for Photoelectrochemical Generation of Hydrogen, *International Journal of Chem. Tech. Research*, **9** (2016), no. 8, 453-464.
- [14] G. Rajakumar, A.A. Rahuman, B. Priyamvada, V.G. Khanna, D.K. Kumar, P.J. Sujin, Eclipta prostrata leaf aqueous extract mediated synthesis of titanium dioxide nanoparticles, *Materials Letters*, **68** (2012), 115-117. <https://doi.org/10.1016/j.matlet.2011.10.038>
- [15] M. Gupta, V. Sharma, J. Shrivastava, A. Solanki, A.P. Singh, V.R. Satsangi, S. Dass, R. Shrivastav, Preparation and characterization of nanostructured ZnO thin films for photoelectrochemical splitting of water, *Bull Mater Sci.*, **32** (2009), no. 1, 23–30. <https://doi.org/10.1007/s12034-009-0004-1>
- [16] M. Vargas, Y. Ochoa, Y. Ortegón, P. Mosquera, J. Rodríguez, R. Camargo, Nanopartículas de TiO₂, fase anatasa, sintetizadas por métodos químicos, *Ingeniería y Desarrollo*, **29** (2011), no. 2, 186–201.
- [17] Z. Li, B. Hou, Y. Xu, D. Wu, Y. Sun, W. Hu, F. Deng, Comparative study of sol-gel-hydrothermal and sol-gel synthesis of Titania-Silica composite nanoparticles, *Journal of Solid State Chemistry*, **178** (2005), no. 5, 1395-1405. <https://doi.org/10.1016/j.jssc.2004.12.034>
- [18] C. Diaz, W. Vallejo, F. Martínez, Synthesis and characterization of TiO₂ thin films doped with copper to be used in photocatalysis, *Iteckne*, **10** (2013), 16-20. <https://doi.org/10.15332/iteckne.v10i1.188>
- [19] P. Dashora, C. Ameta, R. Ameta, S.C. Ameta, Dye-Sensitized Solar Cell Using Copper and Nitrogen Co-doped Titania as Photoanode, *International Journal of Sustainable and Green Energy*, **4** (2015), no.6, 219-226.
- [20] R.S. Varma, B. Baruwati, J. Virkutyte, Doped titanium dioxide as a visible and sun light photo catalyst – US 8,791,044 B2. Washington, DC (US): United States Patent, 2014.

- [21] C.Y. Tsai, H.C. Hsi, T.H. Kuo, Y.M. Chang, J.H. Liou, Preparation of Cu-doped TiO₂ photocatalyst with thermal plasma torch for low-concentration mercury removal, *Aerosol and Air Quality Research*, **13** (2013), no. 2, 639-648. <https://doi.org/10.4209/aaqr.2012.07.0196>
- [22] Université de Namur. Energy table for EDS analysis. Available at: <https://www.unamur.be/services/microscopie/sme-documents/Energy-20table-20for-20EDS-20analysis-1.pdf>. [Accessed 26 Jul. 2017].
- [23] Ingrid Johanna Puentes-Cárdenas, Griselda Ma. Chávez-Camarillo, César Mateo Flores-Ortiz, María del Carmen Cristiani-Urbina, Alma Rosa Netzahuatl-Muñoz, Juan Carlos Salcedo-Reyes, Aura Marina Pedroza-Rodríguez and Eliseo Cristiani-Urbina, Adsorptive Removal of Acid Blue 80 Dye from Aqueous Solutions by Cu-TiO₂, *Journal of Nanomaterials*, **2016** (2016), 1-15. Article ID 3542359. <https://doi.org/10.1155/2016/3542359>
- [24] R. López, R. Gómez, Band-gap energy estimation from diffuse reflectance measurements on sol-gel and commercial TiO₂: a comparative study, *Journal of Sol-Gel Science and Technology*, **61** (2012), no. 1, 1-7. <https://doi.org/10.1007/s10971-011-2582-9>
- [25] J. Navas, A. Sánchez-Coronilla, N.C. Hernández, D.M. De los Santos, J. Sánchez-Márquez, D. Zorrilla, C. Fernández-Lorenzo, R. Alcántara, J. Martín-Calleja, Experimental and theoretical study of the electronic properties of Cu-doped anatase TiO₂, *Phys. Chem. Chem. Phys.*, **16** (2014), no. 8, 3835-3845. <https://doi.org/10.1039/c3cp54273d>
- [26] Y. Wang, R. Zhang, J. Li, L. Li, S. Lin, First-principles study on transition metal-doped anatase TiO₂, *Nanoscale Research Letters*, **9** (2014), no. 46. <https://doi.org/10.1186/1556-276x-9-46>
- [27] M. Guo, J. Du, First-principles study of electronic structures and optical properties of Cu, Ag, and Au-doped anatase TiO₂, *Physica B: Condensed Matter*, **407** (2012), no. 6, 1003-1007. <https://doi.org/10.1016/j.physb.2011.12.128>

Received: December 1, 2017; Published: December 19, 2017